When a pH-triggered nanopatterned shape transition drives the wettability of a hierarchically self-organized film: a bio-inspired effect of "sea Anemone"

Pierre Marcasuzaa, Maud Save, Pierre Gerard, Laurent Billon

When a pH-triggered nanopatterned shape transition drives the wettability of a hierarchically self-organized film: a bio-inspired effect of "sea Anemone"

Pierre Marcasuzaa,[a,b] Maud Save,[a] Pierre Gérard,[c] and Laurent Billon[a,b] *

[a]Universite de Pau & Pays Adour, E2S UPPA, CNRS, IPREM UMR 5254, , 2 avenue du Président Angot, Pau F-64053, France

[b]Bio-inspired Materials Group : Functionalities & Self-assembly, Universite de Pau et Pays Adour, 2 avenue du Président Angot, Pau F-64053, France

[c] Arkema, Groupement de Recherches de lacq, RN 117, 64170 Lacq, France

*Corresponding author. Laurent Billon at Universite de Pau et Pays Adour, Bio-inspired Materials Group : Functionalities & Self-assembly, 2 avenue du Président Angot, Pau F-64053, France, E-mail: laurent.billon@univ-pau.fr (Phone : 00 33 5 59 40 76 09 ; Fax : 00 33 5 59 40 76 23)

Abstract

Hypothesis

Hierarchically structured surfaces including sensitive materials presents the advantage to exalt wettability variation due to the combination of micro structure effect directed by Cassie Baxter and/or Wenzel behaviour which is tuned by the surface energy variation of sensitive polymer films.

Experiments

Herein is reported the synthesis and the hierarchical structuration of a pH sensitive diblock copolymer P(S-*stat*-MMA)-*b*-P4VP with a pH-sensitive Poly 4-vinylpyridine P4VP block. Applying the Breath Figure method casting (minute time scale process), this diblock copolymer allows to obtain a micro porous honeycomb film while a wall nano-structuration due to self-assembly of diblock copolymer is observed.

Findings

The pH-triggered wettability is studied and correlated with the morphology evolution of P4VP nano-domains investigated by AFM in a liquid cell. Indeed, a nano-dots to nano-rings/donuts transition is highlighted when decreasing the pH below the *pK*a of the P4VP. This nano "sea Anemone" shape transition induces the macroscopic changes of the wettability of a hierarchically self-organized honeycomb film, explained by the protonation of P4VP chains inducing electrostatic repulsion and then hydrophilic surface.

Keywords: Hierarchical structure, pH sensitive surface, wettability, micro and nano structuration, Honeycomb film

Introduction

Sensitive materials able to switch properties according to different triggers as temperature, pH, light [1,2] are widely developed for a large range of application as drug delivery, antifogging, self-cleaning or tissue engineering [3,4]. Among them, the switch from hydrophilic to hydrophobic form of polymeric surfaces is quite challenging and interesting [5]. Different polymer families were identified as polyPEG or polyNIPAM sensitive to temperature [6,7], polyazobenzene to light [8–11], polyamine to CO_2 [12–14] or polyacid and polybase to pH [15–17]. However, in case of hydrophilic polymer, the problem of polymer surface solubility in water appears, but can be overcome by using amphiphilic diblock copolymers combining hydrophobic and switchable blocks, *i.e.* hydrophobic/hydrophilic, respectively. Moreover, wettability effect can be enhanced using porous film by reducing the contact surface and more particularly if the change from hydrophilic towards hydrophobic forms is completed by a wettability transition from non-wetting Cassie Baxter to wetting Wenzel states [18].

To combine these two effects, the present work consisted on the elaboration of a hierarchically self-organized film presenting a double structure: the first one at the macroscopic scale, as a porous honeycomb structure, and the second one at the nanoscale as nano-segregation of a diblock copolymer. Herein, a fast bottom-up process based on solvent evaporation in humid atmosphere, so-called “breath figure” process, was used to create the first level of porosity. The directed self-assembly in "breath figure" templating of block copolymers was then able to target the second one by using an amphiphilic diblock [15,19–23]. A P4VP block was chosen as pH sensitive polymer for its ability to switch wettability properties according to the media. Indeed, the protonation of pyridine moiety below its *pK*a [24] introduces some intra/inter electrostatic repulsions in the polymers chains provoking simultaneously a transition from a hydrophobic to hydrophilic surface and then a decrease of

the contact angle value. This macroscopic behaviour is attributed to the re-organization of the P4VP nano-dots into nano-rings domains as a nano "sea Anemone" effect. Indeed, here the mimicry between the nano to macroscopic scale is made by comparison of the macromolecular chains and the sea anemone tentacles behaviors. The P4VP chains behaviour can be compared to sea anemone tentacles which can be collapsed on its mouth, *i.e.* nano-dots (Figure 1a & c), or stretched around the mouth, *i.e.* nano-rings (Figure 1b & d) just by a modification of their close environment.

Materials and methods

To combine hierarchical structure and pH sensitive surface, the synthesis of an amphiphilic diblock copolymer with hydrophilic P4VP and hydrophobic P(S-*stat*-MMA) blocks was performed.

The Styrene S allowed a good control of the MMA polymerization [25]. Thus, a well-defined high molar mass P(S-*stat*-MMA)-b-P4VP copolymer was synthesized by nitroxide-mediated polymerization (NMP) [26] with a number average molecular weight Mn of 48,300 $g.mol^{-1}$ and a dispersity value Đ of 1.29 with a symmetrical molar mass distribution (ESI Figure SI 1, 2 & 3). The final composition of the purified copolymer is of 78% of P(S-*stat*-MMA) and 22% P4VP in volume as measured by ^{1}H NMR in $CDCl_3$.

P(S-*stat*-MMA)-*b*-P4VP copolymer structure allowed manufacturing honeycomb films by the "Breath Figure" method [27]. This method consisted on a fast evaporation of solvent under humidity [28,29]. In case of amphiphilic diblock copolymer, polymer solution is casted on a glass lamella and placed under humid air flow. While the solvent was evaporated (endothermic phenomena), the temperature of the solution decreased and induced

condensation of surrounding humidity at the liquid/air interface. Thus, the hydrophilic part allowed the stabilization of droplet while hydrophobic segment precipitated with water and formed an anti-coalescence layer by a so-called “bag-effect”. Then, droplet self-organized in hexagonal structure due to Bénard-Marangoni convection [30]. After total evaporation of the solvent and water, a porous honeycomb structure was obtained by water droplet templating.

Results and discussion

Hierarchical structure characterization

Micro structure: honeycomb porosity

Micro structure of honeycomb films was checked by optical microscopy which revealed porous surface (ESI Figure SI 5a). Thus, the different images allowed determining the surface ratio of polymer using two methods. The first one, by manual measurement gave a pores radius of 0.5 µm and a distance between two centres of pores of 1.6 µm. Then, using a basic model considering a diamond joining four pores centre which represented an elementary mesh of network, the surface fraction was done by the ratio between surface area (diamond - pore area) and total area (diamond area). This model gave a value of surface fraction of 0.645 (Scheme 1). This value is comparable with the surface ratio of 0.65 ± 0.01 obtained with an ImageJ threshold treatment describe in ESI.

Nano structure: self-assembly of diblock copolymer

The nano structure was investigated by AFM on continuous and honeycomb films (Figure 1 c & e). Continuous films reveals a surface structuration characteristic of the nano-segregation between P(S-*stat*-MMA) and P4VP blocks. On continuous films, characteristic length between two nano-dots P4VP domains is 50 nm which is in accordance with molecular length of two diblock copolymers containing around 500 units of monomers. Images obtained from diblock copolymer honeycomb reveals a hierarchically structured organization. First of all,

micro porosity observed by optical microscopy is confirmed by AFM (Figure 1e). Nevertheless, the principal aim of this characterization was to visualize the nano-segregation of the block copolymer into the walls between pores (Figure 1e) which is similar with the nano-structuration obtained on continuous films (Figure 1c).

Surface properties

Surface properties of materials were investigated by contact angle measurement. This method allows comparing different states of materials wettability according to the variation of composition or the macro-structuration of polymers. Considering a polymer "A" presenting a contact angle value θ_A, the introduction of a second polymer "B" with a contact angle value θ_B, led to a resulting contact angle θ dependent of the surface ratio of each polymers according to the equation 1.

$$cos\theta = \varphi_A cos\ \theta_A + \varphi_B cos\ \theta_B \qquad \text{(Equation 1)}$$

In case of rough surfaces, the contact angle can be differently affected in accordance with Cassie-Baxter or Wenzel models. The difference between these two models is due to the physical behavior of the surface. With Wenzel model, the droplet covered the entire surface and the contact angle θ^* is led by the roughness r (r = Surface area/Surface area projected on a plane) and the Young contact angle θ (due to the chemical nature of polymer which can be determined from a continuous film), for a final equation equal to $\cos\theta^* = r\cos\theta$. When the roughness is higher enough, the energy needed to cover the surface is more important than the energy with air in pore. Therefore, the droplet rests on the top of ruggedness and the residual contact angle θ^* is led by the surface ratio of polymer φ_s and Young contact angle θ, corresponding to the Cassie-Baxter model:

$$\cos\theta^* = -1 + \varphi_s(\cos\theta + 1) \qquad \text{(Equation 2)}$$

where φ_s is the area in contact with liquid / Total area.

Continuous film wettability

By contact angle investigation, an experimental φ_s (P4VP) = 0.19 was determined using equation 3 with a contact angle of the diblock copolymer equal to 78° while P(S-*stat*-MMA) and P4VP respectively presented contact angle values of 85° and 48°.

$$\varphi_s(P4VP) = \frac{\cos\theta_{copolymer} - \cos\theta_{P(S-stat-MMA)}}{\cos\theta_{P4VP} - \cos\theta_{P(S-stat-MMA)}} \quad \text{(Equation 3)}$$

This value was close to the value of the volume fraction (0.22) that testified that block copolymer was uniformly distributed between bulk and surface. The pH effect on film surface can be tuned by the protonation/deprotonation of the pyridine moiety of P4VP. Diblock copolymer presents an increase of contact angle between 45° to 78° when increasing pH from 1 to 10 (Figure 2). This variation follows a typical titration curve with two plateau on both sides of a transition state around pH 5. This last one is attributed to the P4VP *pK*a value of 5.2. Indeed, above this value, deprotonated amino group are pre-dominant while protonated forms appear below the *pK*a. This protonation leads to the formation of a pyridinium salt which possessed more affinities with water, *i.e.* much hydrophilic form, than deprotonated one, *i.e.* much hydrophobic. Such behavior can explain the pH-triggered modulation of wetting on the continuous film.

Honeycomb film wettability

Whatever the pH is, honeycomb films present contact angle upper than continuous films which are lower than 90° (Figure 2). For contact angle values below than 90°, Wenzel model predicts lower contact angle for porous films than continuous film (Young angle). So, this

model can't be applied for the present system. Considering Cassie-Baxter approach and assuming to keep the same chemical nature of the surface from continuous film and in between pores for honeycomb film, a theoretical value of θ^* can be determined assuming the experimental θ value of a continuous film, φ_s of the porous film (0.65 ± 0.01) and the equation 2.

Theoretical and experimental values are in accordance for pH above 6 where a nice fit is observed with the Cassie-Baxter model (Figure 2). However, below this value, the model diverges from the experimental values which are much lower than the predicted ones. This divergence occurs for the pH values reaching the *pK*a of the P4VP and thus enhancing its hydrophilic polyelectrolyte character. So, for the protonated copolymer, the Cassie-Baxter model cannot be applied. Indeed, considering Cassie-Baxter model, the contact angle experimental values lead to a φ_s of 0.83 while SEM images of a honeycomb film after treatment at pH1 reveals a $\varphi_{s,pH1}$ of 0.63 ± 0.01 close to initial value $\varphi_{s,initial}$ of 0.65 ± 0.01. The non-variation of the surface fraction can be explained by the glassy state of the PMMA block with a glass transition temperature T_g close to 100 °C. Therefore, the increase of the surface fraction cannot be assigned to the modification of micro-structure but to the water penetration into the pores without total wetting due to the air confinement, avoiding then to be in Wenzel model. This phenomenon was already observed in case of pillared surfaces in which one water droplet entering to structure without contact with bottom part due to air confinement [31,32].

For fitting the experimental curve, to consider another model taking into account this parameter and determining the depth of penetration of water into pores is necessary. A model is proposed and used considering the hypothesis that pores were in contact as describe in Scheme 1. So, the pore radius (R) is determined as the half of the distance between to center of pores (d). Thus, it is possible to calculate the pore depth ($2R$-h) where h is the height of

virtual dome covering the pore and dicted by $h = R - \sqrt{R^2 - r^2}$ where *r* corresponds to the radius of virtual dome. The surface fraction φ_s is then calculated by equation 4.

$$\varphi_S = \frac{S_{SA} + S_{WSIP}}{S_{SA} + S_{WSIP} + S_{AC}} \quad \text{(Equation 4)}$$

where S_{SA} is the polymer surface area (top of the film), S_{WSIP} the wetting surface into pore and S_{AC} the air contact area.

In this equation, the polymer surface area is constant, but wetting surface into pore and air contact area depends of the penetration depth (*p*). Expression of wetting surface into pore and air contact area are different if the penetration is higher ($p < R\text{-}h$) or lower ($p > R\text{-}h$) than the pore diameter. These two behaviours are given by equations 5; 6 and 7; 8 (Scheme 1), respectively. Using equation 4, 5, 6, 7 and 8, the φ_s *versus* the penetration depth can be drawn (ESI Figure SI 4). Experimental values of contact angle give an experimental φ_s = 0.83, corresponding to a penetration depth of 1.04 µm. Consequently, the height of air in bottom of pore is estimated to be around 400 nm.

The pH-triggered effect on the surface wettability of the microscopic structure is well understood, but we also wanted to focus on the nanostructure impact by AFM with liquid cell at different pH.

pH effect on P4VP nano domains

In case of continuous films, the contact angle values are close to the non-treated films for high pH, as explained by equation 2. Indeed, a media at pH 10 does not modify the structure of the diblock copolymer self-assembly. Image of the immersed surface reveals a *hexagonal-close-packed hcp* pattern with a characteristic distance of 50 nm between P4VP nano-domains (Figure 1c). However, at pH 1 the domains of P4VP are protonated, showing up a shape

transition to nano-rings or nano-donuts, as a nano ”sea anemone” effect (Figure 1d). Even if the surface structure seems to be totally different from pH10 to pH1, a similar hexagonal nano-pattern is observed in both cases with a characteristic distance between nano-donuts center of 50 nm (Figure 1i). This shape transition of the P4VP nano-domains is attributed to the protonation of P4VP inducing a quaternization and the appearance of positive charges along macromolecular chain [33]. Thus, inter and intra macromolecular chain repulsions are created and provoke the nano-holes at the center of P4VP domains (Figure 1g & h). The chain stretching in the 3D directions induces a decrease of the external distance between P4VP nano-donuts which seem to be almost in contact (Figure 1f & i). A concomitant effect is the strong increase of the height of the P4VP nano-domains to deep holes inside the nano-donuts, from 3 nm at pH=10 to 8 nm at pH=1, respectively (Figure 1i). The P4VP chains stretching by a 2.5 times can be associated to a transition from a collapsed polymer brush in a non-solvent to an extended polymer brush in a good solvent [34]. This pH-triggered shape transition lead to an increase of P4VP surface ratio which can be determined by using the experimental contact angle values in equation 3. The calculated surface ratio of P4VP is then equal to 0.65 (0.19 at pH 10), considering P4VP totally protonated at pH = 1 and its homopolymer contact angle close to 0 (cos ($\theta_{\text{protonated P4VP}}$) close to 1).

Same phenomena were observed on honeycombs films with a switch of morphology into wall (between pores) from self-assembled *hcp* nano-dots pattern to organized nano-donuts pattern for pH above and below *pK*a, respectively (Figure 1e & f respectively pH 10 & pH1 and ESI Figure SI 5 b, c & d, respectively pH 8, pH 6 & pH 4)).

Correlation between the macroscopic and nanoscopic observations allow to well-understand the water penetration into the pores covered by P4VP at low pH. Indeed, growing of P4VP surface ratio lead to a total modification of surface properties and explained the large decrease

of the contact angle values for pH below *pK*a leading to the gap with Cassie Baxter state towards a Wenzel state [33].

Conclusions

In the large area of sensitive surface material already reported in literature [6-17], this work describes the synergy of pH-triggered properties and hierarchal structure obtained using the directed self-assembly in "breath figure" templating of a P(S-*stat*-MMA)-*b*-P4VP block copolymers. This copolymer, with a high χ value close to 6.5 between the P(S-*stat*-MMA) and the pH-sensitive P4VP blocks, drives the formation of the self-assembled P4VP nano-dots into the walls between the micropores and leads to a nano-patterned honeycomb film, as a hierarchically structured surface. Then, a pH sweep from 10 to 1 allows to trigger the wettability of the honeycomb film and reveals a transition from a Cassie Baxter model towards a model considering a partial water penetration into the pores below the P4VP *pK*a. The variation of the wettability properties of P4VP material based is enhanced by the roughness effect induced by the hierarchical organization. This switch of model is explained by AFM observations in liquid cell which revealed an increase of surface ratio of P4VP at low pH. Indeed, due to the intra and inter electrostatic repulsion between P4VP chains, a shape transition from nano-dots to nano-donuts is observed as a nano ”sea anemone” effect without affecting the surface ratio but provokes the increase of the hydrophilicity of the surface and a better wettability. This pH effect on porous film was already observed for other pH sensitive polymer like PAA [17] and a polypeptide [16], but going beyond the synthesis of a new diblock copolymer presenting a pH-triggered hierarchical structure, this work established the correlation of the variation of polymer nano domains from nano dots to nano “sea anemone” shape leading to the macroscopic variation of the contact angle. This pH sensitive porous

material opens a large range of application as adsorption/desorption of species according to pH, use P4VP as a precursor of gold salt reduction or for example use it as grafting function [36] to fix some specific species. For the two last applications, according to pH applied, the morphology of the grafted species can be dots or nano rings.

Funding

ARKEMA is thanked for funding this work and the postdoc fellowship of PM in the framework of the GENESIS project.

Conflicts of interest

The authors declare no conflict/competing interest

References

[1] J.-F. Gohy, Y. Zhao, E.S. Gil, Photo-responsive block copolymer micelles: design and behavior, Chem. Soc. Rev. 42 (2013) 7117–7129.
[2] P. Schattling, F.D. Jochum, P. Theato, Multi-stimuli responsive polymers – the all-in-one talents, Polym. Chem. 5 (2014) 25–36.
[3] P.M. Mendes, Stimuli-responsive surfaces for bio-applications, Chem. Soc. Rev. 37 (2008) 2512–2529.
[4] X. Huang, Y. Sun, S. Soh, Stimuli-Responsive Surfaces for Tunable and Reversible Control of Wettability, Adv. Mater. 27 (2015) 4062–4068.
[5] T. Sun, G. Wang, L. Feng, B. Liu, Y. Ma, L. Jiang, D. Zhu, Reversible Switching between Superhydrophilicity and Superhydrophobicity, Angew. Chemie - Int. Ed. 43 (2004) 357–360.
[6] Y. Ye, J. Huang, X. Wang, Fabrication of a Self-Cleaning Surface via the Thermosensitive Copolymer Brush of P(NIPAAm-PEGMA), ACS Appl. Mater. Interfaces. 7 (2015) 22128–22136.
[7] X. Zhao, G. Shan, Research progress on self-assembly of block copolymers of N-isopropyl acrylamide, Huagong Xuebao/CIESC J. 68 (2017) 535–541.
[8] J.Y. Park, U. Male, D.S. Huh, Reversible change of wettability in poly(??-caprolactone/azobenzene) honeycomb-patterned films by UV and visible light illumination, Polym. Bull. 74 (2017) 4235–4249.
[9] C. Bin Kim, J.C. Wistrom, H. Ha, S.X. Zhou, R. Katsumata, A.R. Jones, D.W. Janes, K.M. Miller, C.J. Ellison, Marangoni instability driven surface relief grating in an azobenzene-containing polymer film, Macromolecules. 49 (2016) 7069–7076.
[10] C. Li, Y. Zhang, J. Ju, F. Cheng, M. Liu, L. Jiang, Y. Yu, In situ fully light-driven switching of superhydrophobic adhesion, Adv. Funct. Mater. 22 (2012) 760–763.
[11] T. Zhang, L.Y.L. Wu, Z. Wang, Smart UV/Visible light responsive polymer surface

switching reversibly between superhydrophobic and superhydrophilic, Surf. Coatings Technol. 320 (2017) 304–310.
[12] H. Yin, A.L. Bulteau, Y. Feng, L. Billon, CO2-induced tunable and reversible surface wettability of honeycomb structured porous films for cell adhesion, Adv. Mater. Interfaces. 3 (2016) 1500623–1500632.
[13] H. Liu, S. Lin, Y. Feng, P. Theato, CO2-Responsive polymer materials, Polym. Chem. 8 (2017) 12–23.
[14] P. Marcasuzaa, H. Yin, Y. Feng, L. Billon, CO2-Driven reversible wettability in a reactive hierarchically patterned bio-inspired honeycomb film, Polym. Chem. 10 (2019) 3751–3757.
[15] P. Escalé, L. Rubatat, C. Derail, M. Save, L. Billon, PH sensitive hierarchically self-organized bioinspired films, Macromol. Rapid Commun. 32 (2011) 1072–1076.
[16] A.S. de León, A. del Campo, J. Rodríguez-Hernández, A. Muñoz-Bonilla, Switchable and pH responsive porous surfaces based on polypeptide-based block copolymers, Mater. Des. 131 (2017) 121–126.
[17] C. Wang, Y. Mao, D. Wang, Q. Qu, G. Yang, X. Hu, Fabrication of highly ordered microporous thin films by PS-b-PAA self-assembly and investigation of their tunable surface properties, J. Mater. Chem. 18 (2008) 683–690.
[18] D. Kim, N.M. Pugno, S. Ryu, Wetting theory for small droplets on textured solid surfaces, Nat. Sci. Reports. 6 (2016) 1–8.
[19] P. Escalé, W. Van Camp, F. Du Prez, L. Rubatat, L. Billon, M. Save, Highly structured pH-responsive honeycomb films by a combination of a breath figure process and in situ thermolysis of a polystyrene-block-poly(ethoxy ethyl acrylate) precursor, Polym. Chem. 4 (2013) 4710–4717.
[20] A. Bertrand, A. Bousquet, C. Lartigau-Dagron, L. Billon, Hierarchically porous bio-inspired films prepared by combining “breath figure” templating and selectively degradable block copolymer directed self-assembly, Chem. Commun. 52 (2016) 9562–9565.
[21] P. Escale, M. Save, L. Billon, J. Ruokolainen, L. Rubatat, When block copolymer self-assembly in hierarchically ordered honeycomb films depicts the breath figure process, Soft Matter. 12 (2016) 790–797.
[22] N. Benoot, P. Marcasuzaa, L. Pessoni, S. Chasvised, S. Reynaud, A. Bousquet, L. Billon, Hierarchically organized honeycomb films through block copolymer directed self-assembly in “breath figure” templating and soft microwave-triggered annealing, Soft Matter. 14 (2018) 4874–4880.
[23] P. Marcasuzaa, S. Pearson, K. Bosson, L. Pessoni, J.C. Dupin, L. Billon, Reactive nano-patterns in triple structured bio-inspired honeycomb films as a clickable platform, Chem. Commun. (Camb). 54 (2018) 13068–13071.
[24] S.R. Narayanan, S.P. Yen, L. Liu, S.G. Greenbaum, Anhydrous proton-conducting polymeric electrolytes for fuel cells, J. Phys. Chem. B. 110 (2006) 3942–3948.
[25] J. Nicolas, C. Dire, L. Mueller, J. Belleney, B. Charleux, S.R.A. Marque, D. Bertin, S. Magnet, L. Couvreur, Living character of polymer chains prepared via nitroxide-mediated controlled free-radical polymerization of methyl methacrylate in the presence of a small amount of styrene at low temperature, Macromolecules. 39 (2006) 8274–8282.
[26] J. Nicolas, Y. Guillaneuf, D. Bertin, D. Gigmes, B. Charleux, Nitroxide-Mediated Polymerization, Polym. Sci. A Compr. Ref. 10 Vol. Set. 3 (2012) 277–350.
[27] G. Widawski, M. Rawiso, B. François, Self-organized honeycomb morphology of star-polymer polystyrene films, Nature. 369 (1994) 387–389.
[28] P. Escalé, L. Rubatat, L. Billon, M. Save, Recent advances in honeycomb-structured

porous polymer films prepared via breath figures, Eur. Polym. J. 48 (2012) 1001–1025.
[29] A. Munoz-Bonilla, M. Fernandez-Garcia, J. Rodriguez-Hernandez, Towards hierarchically ordered functional porous polymeric surfaces prepared by the breath figures approach, Prog. Polym. Sci. 39 (2014) 510–554.
[30] J. Nicolas, L. Mueller, C. Dire, K. Matyjaszewski, B. Charleux, Comprehensive modeling study of nitroxide-mediated controlled/living radical copolymerization of methyl methacrylate with a small amount of styrene, Macromolecules. 42 (2009) 4470–4478.
[31] P. Papadopoulos, L. Mammen, X. Deng, D. Vollmer, H.J. Butt, How superhydrophobicity breaks down, Proc. Natl. Acad. Sci. U. S. A. 110 (2013) 3254–3258.
[32] A. Elbourne, M.F. Dupont, S. Collett, V.K. Truong, X.M. Xu, N. Vrancken, V. Baulin, E.P. Ivanova, R.J. Crawford, Imaging the air-water interface: Characterising biomimetic and natural hydrophobic surfaces using in situ atomic force microscopy, J. Colloid Interface Sci. 536 (2019) 363–371.
[33] L. Wang, F. Montagne, P. Hoffmann, R. Pugin, Gold nanoring arrays from responsive block copolymer templates, Chem. Commun. 25 (2009) 3798–3800.
[34] D. Bendejacq, V. Ponsinet, M. Joanicot, Water-dispersed lamellar phases of symmetric poly(styrene)-block- poly(acrylic acid) diblock copolymers: Model systems for flat dense polyelectrolyte brushes, Eur. Phys. J. E. 3 (2004) 3–13.
[35] D. Murakami, H. Jinnai, A. Takahara, Wetting transition from Cassie-Baxter to Wenzel states on textured surfaces, Langmuir. 30 (2000) 2–4.
[36] E. Poggi, W. Ouvry, B. Ernould, J.P. Bourgeois, S. Chattopadhyay, F. Du Prez, J.F. Gohy, Preparation of Janus nanoparticles from block copolymer thin films using triazolinedione chemistry, RSC Adv. 7 (2017) 37048–37054.

Figures and Scheme captions

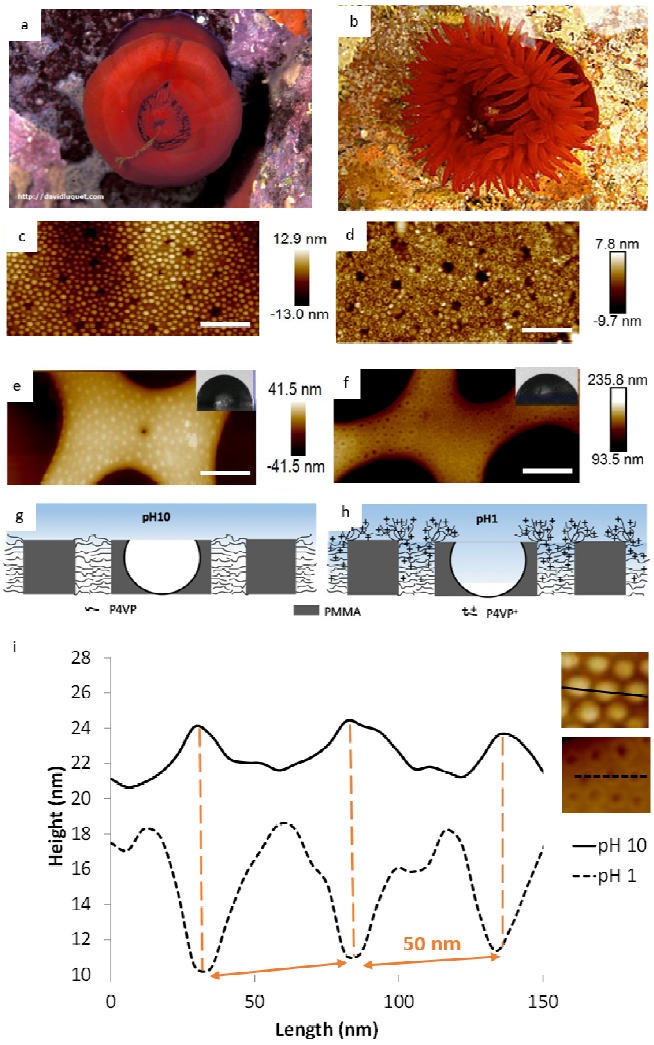

Figure 1 – Sea anemone pictures with collapsed (a) and stretched (b) tentacles. AFM height profile microscopy images (scale bar = 300nm) of continuous film at pH 10 (c) and pH 1 (d) and of honeycomb film at pH 10 (e) pH 1 (f). Schematic representation of neutral and protonated P4VP (g and h). Height & distance profile of P(MMA-stat-S)-b-P4VP nano self-assembly at pH 10 (full line) and pH 1 (dotted line) (i).

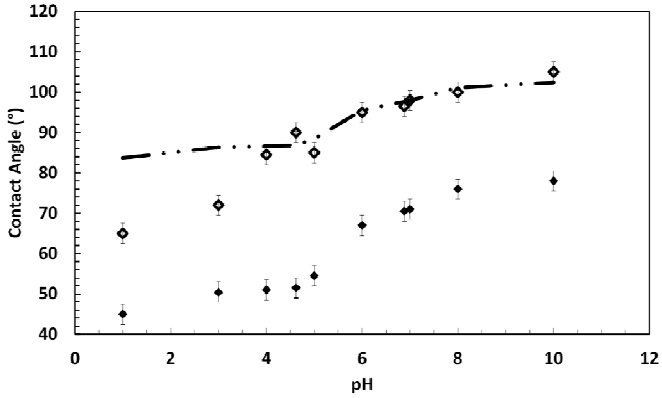

Figure 2 - Contact angle evolution with pH for continuous films (full diamonds) and honeycomb films (empty diamonds). Theoretical value of θ* according to Cassie-Baxter model (dotted line).

1

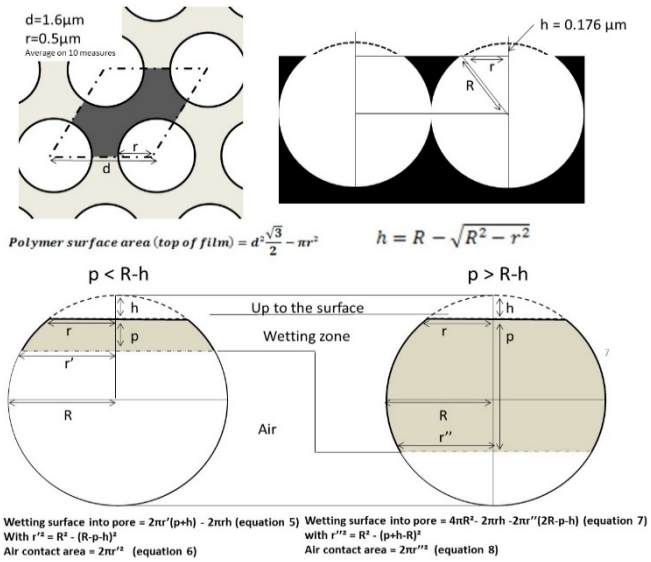

Scheme 1 - Schematic representation of pores with characteristic distances and area used for model applicable in

2 equation 4.

3

4

5

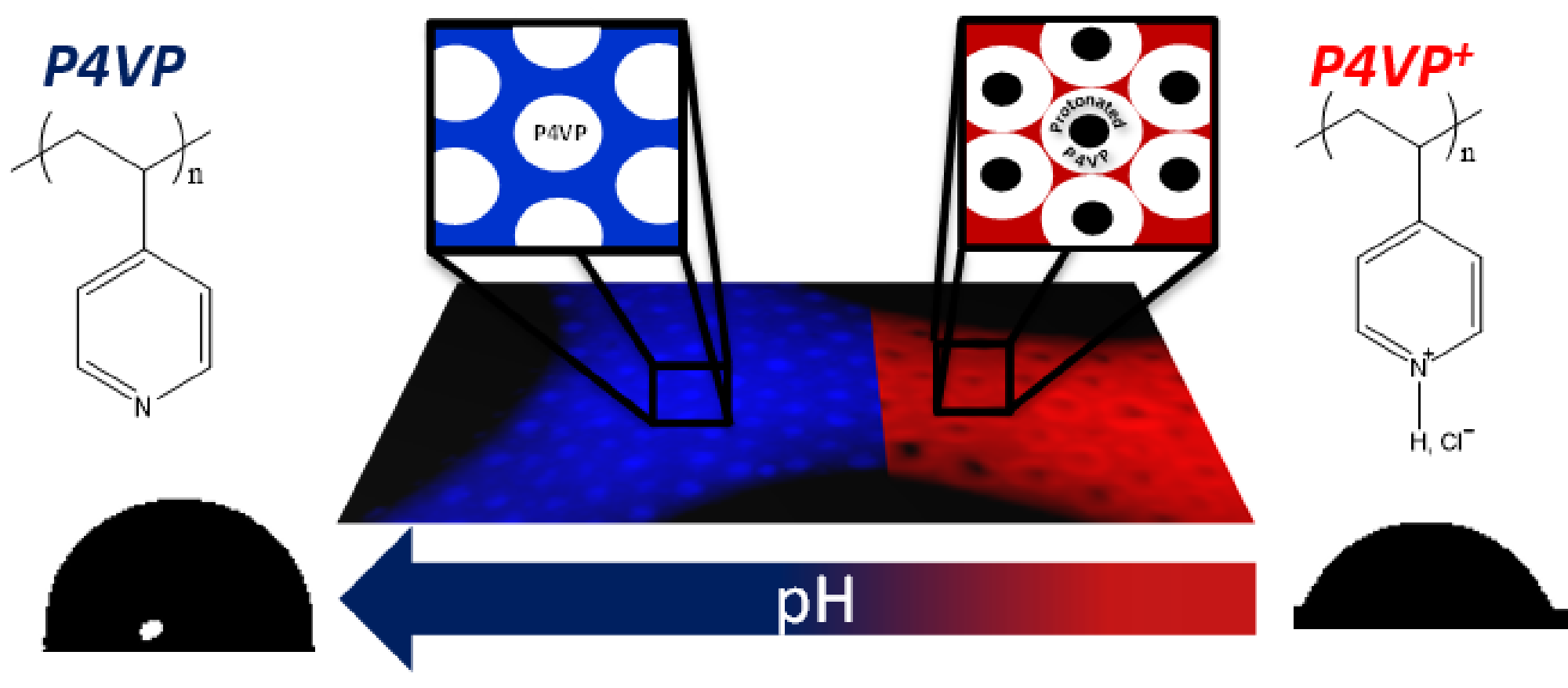
P4VP
n
N
P4VP
Protonated P4VP
P4VP+
n
N+
H, Cl−
pH